1   **The distribution of methylated sulfur compounds, DMS and DMSP, in**

2   **Canadian Subarctic and Arctic marine waters during summer, 2015**

3   Tereza Jarníková [1], John Dacey[2], Martine Lizotte[3], Maurice Levasseur [3]

4   and Philippe Tortell[1,4,5]

5   (1) Department of Earth, Ocean and Atmospheric Sciences, University of British

6   Columbia, 2022 Main Mall, Vancouver BC, Canada V6T 1Z3

7   (2) Woods Hole Oceanographic Institution, Woods Hole, MA 02543.
8

9   (3) Université Laval, Department of Biology (Québec-Océan), Québec City, Québec,

10   Canada.

11   (4) Department of Botany, University of British Columbia, 6270 University Blvd.,

12   Vancouver BC, Canada V6T 1Z4

13   (5) Peter Wall Institute for Advanced Studies, University of British Columbia, 6330

14   Crescent Blvd., Vancouver BC, Canada V6T 1Z4

15   **Correspondence to: Tereza Jarníková (tjarniko@eoas.ubc.ca)**

16   **Abstract**

17   **We present seawater concentrations of dimethylsulfide (DMS), and**

18   **dimethylsulfoniopropionate (DMSP) measured across a transect from the Labrador**

19   **Sea to the Canadian Arctic Archipelago, during summer 2015. Using an automated**

20   **ship-board gas chromatography system, and a membrane-inlet mass spectrometer,**

21   **we measured a range of DMS (~1 nM to 18nM) and DMSP concentrations (~1 nM to**

22   **150 nM) that was consistent with previous observations in the Arctic Ocean. The**

23   **highest DMS and DMSP concentrations occurred in a localized region of Baffin Bay,**

24   **where surface waters were characterized by high chlorophyll *a* (chl *a*) fluorescence,**

25   **indicative of elevated phytoplankton biomass. Across the full sampling transect,**

26   **there were only weak relationships between DMS/P, chl *a* fluorescence and other**

27   **measured variables, including positive relationships between DMSP:chl *a* ratios and**

28   **several taxonomic marker pigments, and elevated DMS/P concentrations in partially**

29   **ice-covered areas. Our high spatial resolution measurements allowed us to examine**

30   **DMS variability over small scales (<1 km), and document strong DMS**

31   **concentration gradients across surface hydrographic frontal features. The new**

32   **observations presented in this study constitute a significant contribution to the**

33   **existing Arctic DMS/P dataset, and provide a baseline for future measurements in**

34   **the region.**

Biogeosciences
Discussions

Open Access

EGU

1. Introduction

35

36   The trace gas dimethylsulfide (DMS), a degradation product of the algal

37   metabolite dimethylsulfoniopropionate (DMSP), is the largest natural source of sulfur to

38   the atmosphere, accounting for over 90% of global biogenic sulfur emissions (Simó,

39   2001). In the atmosphere, DMS is rapidly oxidized to sulfate aerosols that act as cloud

40   condensation nuclei (CCN), backscattering incoming radiation, increasing the albedo of

41   low-altitude clouds and potentially cooling the Earth (Charlson et al., 1987). The seminal

42   CLAW hypothesis proposed by Charlson et al. (1987) suggests that this negative radiative

43   forcing will have cascading effects on marine primary productivity, leading to a DMS-

44   mediated climate feedback loop. Since its publication in 1987, the CLAW hypothesis has

45   provided motivation for the widespread measurement of DMS in the global ocean.

46   Beyond their potential role in regional climate forcing, DMS and DMSP also play

47   critical ecological roles in marine microbial metabolism and food-web dynamics (for a

48   complete overview; see Stefels et al., 2007). DMSP is believed to serve numerous

49   physiological functions in phytoplankton, with suggested roles as an osmolyte, an anti-

50   oxidant, and a cryoprotectant under different environmental conditions. Sunda et al.

51   (2002) suggested that oxidative stressors, such as high solar radiation or iron limitation,

52   may stimulate DMSP production in certain phytoplankton species. The production of this

53   molecule is largely species-dependent, and can vary by three orders of magnitude among

54   phytoplankton groups, with the highest intracellular concentrations typically reported in

55   dinoflagellates and haptophytes, and lower concentrations in diatoms (Keller, 1989).

56   After synthesis, DMSP can be cleaved to DMS and acrylate within algal cells, or

57   by heterotrophic bacteria acting on the dissolved DMSP (DMSP$_d$) pool in the water

58   column (Zubkov et al., 2001). The release of DMSP into the water column is believed to

59   be enhanced in physiologically stressed or senescent phytoplankton (Malin et al., 1998).

60   and can be stimulated by zooplankton grazing and viral lysis (Zubkov et al., 2001).

61   Bacteria can also utilize DMSP$_d$ as a sulfur source for protein synthesis (Kiene et al.,

62   2000), but this pathway does not lead to DMS release. The DMS yield of bacterial

63   DMSP metabolism (i.e. the fraction of consumed DMSP that is converted to DMS) varies

64   significantly, and may be influenced by the relative supply and demand of reduced sulfur

65   and carbon for bacterial growth (Kiene and Linn, 2000).

66   Modeling studies have suggested that DMS emissions could exert an especially

67   significant influence on regional climate in polar regions, due to the low background

68   concentrations of atmospheric aerosols at high latitudes (Woodhouse et al., 2010). In

69   support of this, direct observations have demonstrated a link between particle formation

70   events in the Arctic atmosphere and sea surface DMS emissions (Chang et al., 2011),

71   (Mungall et al., 2016), motivating further quantification of marine DMS emissions in

72   Arctic regions. Yet, logistical constraints have limited the measurements of surface water

73   properties in many high latitude regions, and these areas remain relatively sparsely

74   sampled for DMS/P concentrations. Indeed, of the approximately 50,000 data points in

75   the global Pacific Marine Environmental Laboratory (PMEL) database of oceanic DMS

76   measurements (http://saga.pmel.noaa.gov/dms/), only 5 % have been made in either

77   Arctic or Antarctic waters (~ 1600 and 1000 data points, respectively).

78   Despite the relatively limited sulfur observations in high latitude waters, an

79   examination of the available data reveals large differences in the water column DMS

80   distributions of the Arctic and Antarctic regions. While the summertime mean DMS

81   concentration in the Arctic Ocean is 3.0 nM (close to the global mean value of 4.2 nM,

82   derived from the PMEL data), the mean summertime DMS concentration in the Southern

83   Ocean is ~ 3 times higher at 9.3 nM. Moreover, several areas of extraordinarily high

84   DMS concentrations (>100 nM) have been observed in various regions of the Southern

85   Ocean (DiTullio et al. 2000; Tortell et al. 2011), whereas no study to date has observed

86   DMS concentrations above 25 nM in Arctic waters. The available data thus suggest

87   contrasting dynamics of DMS/P production in the two polar regions (i.e. Arctic vs.

88   Antarctic).

89   Although Arctic and Antarctic regions share several key physical characteristics,

90   most notably strong seasonal cycles in sea ice cover and solar irradiance, there are some

91   critical differences. Much of the pelagic Southern Ocean is an iron-limited, High

92   Nutrient Low Chlorophyll (HNLC) regime, with strong seasonal changes in mixed layer

93   depths (Boyd et al., 2001). Low iron conditions, and seasonally-variable mixed layer

94   light levels may induce oxidative stress (particularly in ice-influenced stratified waters)

95   and thus promote high DMS production (Sunda et al., 2002). In addition, parts of the

96   Southern Ocean are characterized by extremely high biomass of *Phaeocystis antarctica*

97   (Smith et al., 2000), a colonial haptophyte that is a prodigious producer of DMSP and

98   DMS (Stefels et al., 2007). By comparison, the salinity-stratified surface waters of the

99   Arctic Ocean are believed to be primarily limited by macronutrient (i.e. nitrate)

100   availability (Tremblay et al., 2006), with a maximum phytoplankton biomass that is at

Biogeosciences
Discussions

Open Access

EGU

101   least an order of magnitude lower than that observed in the Southern Ocean (Carr et al.,

102   2006). Despite the relatively low phytoplankton biomass over much of the Arctic Ocean,

103   reasonably high summertime DMS levels (max ~ 25 nM) have been observed in some

104   regions. It is also important to note that significant Arctic phytoplankton biomass and

105   primary productivity may occur in sub-surface layers (Martin et al. 2010), and in under-

106   ice blooms (Arrigo et al., 2012). The quantitative significance of these blooms for DMS

107   production is unknown at present (Galindo et al., 2014).

108   Quantifying the spatial and temporal distribution of DMS and DMSP in the Arctic

109   Ocean is particularly important in light of the rapidly changing hydrographic conditions

110   across this region. Rapid Arctic warming over the past several decades has been

111   associated with a significant reduction in the extent of summer sea ice, resulting in higher

112   mixed layer irradiance levels and a longer phytoplankton growing season (Arrigo et al.,

113   2008). Arrigo et al (2008) suggested that continued warming and sea-ice loss could lead

114   to a three-fold increase in primary productivity over the coming decades. The effects of

115   these potential changes on DMS/P concentrations and cycling remain unknown, but it has

116   been suggested that future changes in Arctic Ocean DMS emissions could modulate

117   regional climatic patterns (Levasseur, 2013). Indeed, modeling work has suggested that

118   cooling associated with increased DMS production and emissions in a less ice-covered

119   Arctic may help offset warming associated with loss of sea-ice albedo (Gabric et al.,

120   2004). The important climatic and biological roles of reduced sulfur compounds,

121   combined with altered marine conditions under a warming environment, provide the

122   motivation for a deeper understanding of the distribution and cycling of DMS and related

6

Biogeosciences
Open Access
Discussions
EGU

123   compounds in Arctic waters.

124   In this article, we present a new data set of DMS and DMSP concentrations in

125   Arctic and Subarctic waters adjacent to the Canadian continental shelf. We used a

126   number of recent and emerging methodological approaches to measure these compounds

127   in a continuous ship-board fashion. In particular, we used membrane inlet mass

128   spectrometry (MIMS) to measure DMS with extremely high spatial resolution (i.e. sub-

129   km scale), and the recently developed organic sulfur sequential chemical analysis robot

130   (OSSCAR), for automated analysis of DMS and DMSP. Our goal was to utilize the

131   sampling capacities of the MIMS and OSSCAR systems to make simultaneous

132   measurements of DMS/P in Subarctic Atlantic and Arctic waters, in order to expand the

133   spatial coverage of the existing DMS/P dataset, and identify environmental conditions

134   leading to spatial variability in the concentrations of these compounds.

135   **2. Methods**

136   **2.1 Study Area**

137   Our field study was carried out on board the *CCGS Amundsen* during Leg 2 of the 2015

138   GEOTRACES expedition to the Canadian Arctic, (July10 – August 20, 2015). We

139   sampled along a ~ 10,000 km transect from Quebec City, Quebec, to Kugluktuk,

140   Nunavut. Data collection commenced off the coast of Newfoundland, and included

141   waters of the Labrador Sea, Baffin Bay and the Canadian Arctic Archipelago (Fig. 1).

142   The cruise transect covered two main distinct geographic domains – the Baffin

143   Bay/Labrador Sea region, and the Canadian Arctic Archipelago (CAA). The majority of

144   the surface water in the Canadian Arctic Archipelago is from Pacific-sourced water

145   masses, as a shallow sill near Resolute limits the westward flow of Atlantic-sourced water

146   (Michel et al., 2006). Flow paths through the CAA are complex. The region is

147   characterized by a network of shallow, narrow straits that are subject to significant

148   regional variability in local mixing and tidal processes, and strongly influenced by

149   riverine input, which drives stratification (Carmack et al, 2011). By contrast, both

150   Atlantic- and Pacific-sourced waters mix in the Baffin Bay and Labrador Sea regions, and

151   this confluence drives a strong thermohaline front. These regions are less strongly

152   stratified than the CAA (Carmack et al, 2011).

153   **2.2 Underway sampling systems**

154   We utilized two complementary underway sampling systems to measure reduced

155   sulfur compounds; membrane inlet mass spectrometry (MIMS; Tortell, 2005)), and the

156   organic sulfur sequential chemical analysis robot (OSSCAR; Asher et al., 2015)).

157   Detailed methodological descriptions of these systems have been published elsewhere

158   ((Tortell, 2005, 2011), (Asher et al., 2015)), and only a brief overview is given here.

159   **2.2.1 OSSCAR**

160   The OSSCAR instrument consists of an automated liquid handling / wet

161   chemistry module that is interfaced to a custom-built purge-and-trap gas chromatograph

162   (GC) equipped with a pulsed flame photometric detector (PFPD) for sulfur analysis. A

163   custom LabVIEW program is used to automate all aspects of the sample handling and

164   data acquisition. During analysis, unfiltered seawater (3 - 5 ml) from an underway supply

165   (nominal sampling depth ~ 5 m) is drawn via automated syringe pump into a sparging

166   chamber. DMS is then stripped out of solution (4 minutes of 50 ml min^{-1} N$_2$ flow) onto a

8

Biogeosciences
Discussions

Open Access

EGU

167   1/8" stainless steel trap packed with carbopack at room temperature. Rapid electrical

168   heating of the trap (to ~260°C), causes DMS desorption onto a capillary column (Restek

169   SS MXT, 15m, 80 °C, 2 ml min^{-1} N$_2$ flow) prior to detection by the PFPD (OI Analytical,

170   Model 5380). Light emitted during combustion in the PFPD is converted to a voltage and

171   recorded by a custom built Labview data acquisition interface. Following the completion

172   of DMS analysis, 5 N sodium hydroxide is added to the sparging chamber for 14 minutes

173   to cleave DMSP in solution to DMS, following the method of Dacey and Blough (Dacey

174   and Blough, 1987). The resulting DMS is sparged out of solution and measured as

175   described above. The sparging chamber is then thoroughly rinsed with Milli-Q water,

176   and the process can be repeated. As we used unfiltered seawater for our analysis, it is

177   important to note that we measured total DMSP (DMSP$_t$) concentrations, which represent

178   the sum of dissolved and particulate pools.

179   We measured an in-line standard every 4-5 samples (at most every 3 hours) to

180   ensure that the system was functioning correctly, and to correct for potential detector

181   drift. The mean standard error of daily point standards was 0.55 nM, and we consider

182   this to represent the precision of our emerging method (significant efforts are underway

183   to increase this precision). To correct the underway data for instrument drift, point

184   standard measurements were smoothed with a 3-pt running mean filter, interpolated to the

185   time-points of sample measurements, and compared to the known standard concentration

186   to provide a drift correction factor for every seawater data point. Six-point calibration

187   curves were performed every two days, using DMS standards (ranging from 0 to 18nM),

188   produced from automated dilutions of a primary DMS stock and Milli-Q water (see Asher

189   et al., 2015). The limit of detection of the system was calculated from the calibration

190   curve using the formula $C_{LOD} = 3s_{y/x} \div b$, where C_{LOD} is the concentration limit of

191   detection, $s_{y/x}$ is the standard error of the regression , and b is the slope of the regression

192   line. With this approach, we derived a mean limit of detection of 1.4 nM. The mean

193   linear calibration curve R^2 value, taken over all calibration curves, was 0.9887.

194   The OSSCAR system is designed to automate the collection of seawater for

195   sequential analysis of DMS, DMSO, and DMSP in a single sample. During our cruise,

196   however, we experienced problems with the DMSO reductase enzyme used to convert to

197   DMS for analysis, and we therefore configured the instrument to run only DMS and

198   DMSP at sea, with one cycle requiring roughly 30 minutes.

199   **2.2.2 MIMS**

200   We used Membrane Inlet Mass Spectrometry (MIMS) to obtain very high frequency

201   measurements (~ several data points per minute) of DMS concentrations and other gases

202   in surface seawater. Using this system, seawater from the ship's underway loop was

203   pumped through a flow-through sampling cuvette, attached, via a silicone membrane, to a

204   quadrupole mass spectrometer (Hiden Analytical HPR-40). DMS was measured by

205   detecting ions with a mass to charge ratio of 62 (m/z 62) every ~30 seconds. To achieve

206   constant sample temperature prior to contact with the membrane, seawater was passed

207   through a 20 foot coil of stainless steel tubing immersed in water bath held at 4 °C

208   (Tortell et al. 2011). The system pressure (as measured by the Penning Gauge) remained

209   stable during operation (~1.3 – 1.5 x 10 ^(-6) Torr). The DMS signal was calibrated using

210   liquid standards that were produced by equilibrating 0.2 μm filtered seawater with a

211   constant supply of DMS (m/z 62) from a calibrated permeation device (VICI Metronics).

212   The primary effluent from the permeation tube (held at 30 °C) was split among several

213   capillary outflows and mixed into a N_2 stream ($\sim$ 50 ml min^{-1}) to achieve a range of

214   DMS / N_2 mixing ratios for bubbling into standard bottles held in an incubator tank

215   supplied with continuously flowing seawater. Concentrations of DMS in the standard

216   bottles were cross-validated by measuring discrete samples using the OSSCAR system.

217   **2.3 Post-processing of DMS data**

218   Raw data outputs (voltages) for both OSSCAR and MIMS measurements were processed

219   into final concentrations using MATLAB scripts. For OSSCAR data, raw voltages were

220   captured with a sampling frequency of 5 Hz. Sulfur peaks eluting off the GC column

221   were integrated using a custom MATLAB script, with correction for baseline signal

222   intensities.   DMS concentrations were derived from peak areas using the calibration

223   curves as described above.

224   **2.4 Ancillary seawater data**

225   Shipboard salinity, temperature, wind speed, and chlorophyll *a* (chl *a*)

226   fluorescence measurements were collected using several underway instruments. We used

227   a Seabird Electronics thermosalinograph (SBE 45) for continuous surface temperature

228   and salinity measurements, and a Wetlabs Fluorometer (WetStar) to measure chl *a*

229   fluorescence, as a proxy for phytoplankton biomass. We note that the chl *a* fluorescence

230   data are subject to significant diel cycles associated with light-dependent fluorescence

231   quenching. All sensors were calibrated prior to and following the summer expedition.

232   Conductivity Temperature Depth (CTD) profiles were used to measure vertical profiles of

233   salinity and potential temperature at 17 stations, from which we computed density using

234   the Seawater Toolbox in MATLAB. The mixed layer depth was defined as the depth

235   where density exceeded surface values by 0.125 kg m^{-3}. Sea ice concentrations were

236   obtained from the AMSR-E satellite product (Cavelieri et al. 2006) with a spatial

237   resolution of 12.5 km. The percent ice cover along the cruise track was derived from a

238   two dimensional interpolation of the ship's position in time and space against the daily

239   sea ice data.

240   All correlation analyses (Pearson's r) were computed in MATLAB, using the

241   corrcoef function. Sample sizes were as follows: 33,250 data points in the MIMS DMS

242   dataset, 344 in the OSSCAR DMS dataset, and 318 in the OSSCAR DMSP dataset.

243   **2.5 Phytoplankton biomass and taxonomic composition**

244   In addition to underway data, samples for the quantification of photosynthetic and

245   accessory pigments (Table 1) were collected at a number of discrete oceanographic

246   stations (see Table 2). For each station, duplicate samples (250-500 mL) for chl *a* analysis

247   were filtered onto pre-combusted 25 mm glass fiber filters (Whatman GF/F) using low

248   vacuum pressure (<100 mm Hg). Filters were stored at -20 ºC and chl *a* was determined

249   within a few days of sample collection using fluorimetric analysis following the method

250   of Welschmeyer (Welschmeyer 1994). Duplicate 1-2 L samples were filtered onto pre-

251   combusted 25 mm GF/F for pigment analysis by reverse-phase High-Performance Liquid

252   Chromatography (HPLC). Filters were dried with absorbent paper, flash frozen in liquid

253   nitrogen and stored at -80 ºC until analysis following the method of Pinckney et al

254   (1994). We used several diagnostic pigments as markers for individual phytoplankton

255   groups, as described by Coupel et al (2015) (see Table 1). Following HPLC pigment

256   processing, data were interpreted with the chemotaxonomy program CHEMTAX V1.95,

257   using the pigment ratio matrix described by Taylor et al (2013).

258   **2.6 DMS Sea-Air Flux**

259   We derived sea-air fluxes of DMS from MIMS measurements of DMS

260   concentrations, as these data had higher resolution and spatial coverage than OSSCAR

261   observations. We computed sea-air flux as:

262    $$F_{DMS} = k_{DMS} \, (DMS_{SW}) \, (1 - A)^{0.4} \qquad (1)$$

263   Where DMS_{sw} is the concentration of DMS in the surface ocean and k_{DMS} is the gas

264   transfer velocity derived from the equations of Nightingale et al. (2000), normalized to

265   the temperature and salinity-dependent DMS Schmidt number of Saltzman et al. (1993).

266   The term A represents percent sea ice cover, and the scaling exponent of 0.4 accounts for

267   the effects of sea ice on gas exchange and is derived from the work of Loose et al. (2009).

268   Sea surface salinity and temperature measurements described in section 2.5 were used in

269   the calculations. Wind speed data were obtained from the ship's anemometer (AAVOS

270   data, Environment Canada).

271   **3. Results**

272   **3.1 Oceanographic setting**

273   Figures 1 and 2 show the distribution of hydrographic properties across our cruise

274   survey region. Over our sampling area, surface water temperatures varied between -1.2

275   and 10.2 °C, while surface salinity ranged from 10.7 to 34.7 psu (Fig. 1). The warmest

276   and most saline waters were found in the Labrador Sea, with cold fresher waters in

13

277   Hudson Strait and the Canadian Arctic Archipelago. Underway chl *a* fluorescence varied

278   between 0.04 and 2.96 µg L^{-1}, averaging 0.20 µg L^{-1}. The highest chl *a* fluorescence was

279   observed in a localized region within Baffin Bay, in the vicinity of a sharp temperature

280   and salinity frontal zone (Fig. 1). Mixed layer depths ranged from ~ 5 - 50 m, and were

281   deepest in the Labrador Sea and shallowest in the stations of the Canadian Arctic

282   Archipelago. Sea ice cover was variable across the survey transect, with ice-free waters

283   in the Labrador Sea, and significant ice cover in the northern Hudson Bay and parts of the

284   Canadian Arctic Archipelago (Fig. 2).

285   **3.2 Phytoplankton biomass and taxonomic distributions**

286   Using measurements of accessory photosynthetic pigments, we examined spatial patterns

287   in the taxonomic composition of phytoplankton assemblages (see Table 1 for a

288   description of HPLC marker pigments and their associated phytoplankton taxa).The

289   distribution of pigments across our sampling stations is presented in Table 2, along with

290   measurements of mixed layer depth and ice cover, while CHEMTAX-derived assemblage

291   estimates are shown in Table 4. In order to remove large potential differences in total

292   phytoplankton biomass, we normalized pigment concentrations to total chl a

293   concentrations measured using HPLC (see Methods, section 2.5).

294   CHEMTAX pigment analysis shows that all stations in the study area were diatom-

295   dominated, although haptophyte, dinoflagellate, and prasinophyte markers were detected

296   in varying quantities at all stations (see Table 4). Total HPLC-measured chl *a* was

297   relatively low throughout the study area, ranging from 0.11 to 0.56 µgL^{-1}.

298   **3.3 Observed DMS/P concentration ranges**

14

299   The DMS data shown in Fig. 1 are derived from MIMS measurements, since

300   these have wider geographic coverage and greater spatial resolution than OSSCAR data.

301   DMS concentrations measured with MIMS ranged from 0.2 nM to 12 nM, averaging 2.7

302   (± 1.5) nM. The highest values were observed in the northern Labrador Sea, Baffin Bay

303   and Hudson Strait, with lower values through much of the Arctic Archipelago.

304   Figure 3 shows the distribution of DMS, measured by both MIMS and OSSCAR,

305   along the cruise track. DMS concentrations measured with OSSCAR ranged from 0.1 to

306   18nM, averaging 3.2± 2.4nM. In general, we observed reasonably good coherence

307   between DMS measurements made by our two analytical systems, with similar absolute

308   values of data and spatial patterns. There were, however, notable offsets in the early

309   August measurements (~ km 7000 cruise track, Fig. 3a), when OSSCAR DMS data were

310   consistently higher than MIMS data. Notwithstanding this offset (for which potential

311   reasons are addressed in the discussion), the good coherent spatial patterns in data

312   derived from these independent methods is encouraging, particularly given the rather low

313   precision of our current OSSCAR system.

314   The spatial distribution of DMSP concentrations (measured with OSSCAR) along

315   the cruise track is also shown in Fig. 3. Concentrations ranged from <1 nM to 160 nM,

316   and averaged 30 ± 29nM. DMSP:chl a ratios measured from HPLC chl a data ranged

317   from 52.31nmol μg^(-1) to 181.4nmol μg^(-1). Examination of the data in Figure 3

318   reveals that high DMS concentrations were sometimes, but not always, accompanied by

319   high DMSP concentrations. For example, a sharp increase in measured DMSP

320   concentrations (around 7000-7400 km) on the cruise track was accompanied by a sharp

15

321   increase in DMS measured by both instruments, while low-DMS waters observed around

322   km 9400 along the transect also showed very little DMSP. Over the portion of the

323   transect where measurements of both DMS and DMSP were available, the OSSCAR-

324   measured concentrations of these compounds exhibited a statistically significant positive

325   correlation ($r = 0.52$, $p < 0.001$). There were, however, a number of regions where

326   increased DMS concentrations were not accompanied by increases in DMSP (e.g. ~ km

327   10,000).

3.4 Sea-Air Flux

329   Figure 5 shows DMS sea-air fluxes as computed from MIMS-measured DMS seawater

330   concentrations, wind speed and sea ice cover. DMS sea-air fluxes ranged from < 1 to 80

331   μmol S m^{-2} day^{-1}, with peak sea-air flux observed around km 5500 on the cruise track.

332   Sea-air flux is highly dependent on wind speed and sea ice cover, with the result that even

333   high concentrations of seawater DMS yielded low sea-air flux when low wind and/or

334   high sea ice was present (e.g. km 2100, 7200, 8300). Conversely, very high sea-air fluxes

335   were observed when moderately high DMS concentrations coincided with high wind

336   speeds and ice-free waters (e.g. km 5400).

3.5 Comparison of gradients in DMS data with hydrographic features

338   The high sampling frequency of MIMS measurements allows the comparison of

339   DMS observations with other underway environmental variables, and enables the

340   quantification of small-scale DMS concentration gradients in near real-time. Figure 2

341   shows a cruise track record of MIMS-measured DMS concentrations in relation to

342   salinity, temperature, chl *a* fluorescence, and ice cover. Several sharp increases in DMS at

16

343   around kms 2100, 3300, and 3800 along the cruise track were accompanied by strong

344   gradients in temperature and, to a lesser extent, salinity (Fig. 2). These regions

345   correspond to areas in the Labrador Sea and Baffin Bay. An increase in DMS

346   concentrations in Baffin Bay around km 7200 in the cruise track (Fig 2a) was associated

347   with a simultaneous drop in sea-surface temperature and salinity, in close proximity to a

348   sharp increase in chl *a* fluorescence along the cruise track (Fig 2c) (see Fig. 1). As shown

349   in Fig 3b, this localized region exhibited the highest concentrations of DMSP along the

350   transect. Interestingly, this area was also characterized by strong gradients in sea ice

351   concentrations, and the low salinity waters are indicative of localized ice melt. Figures 1d

352   and 2d also show the large-scale salinity gradients in the Hudson Bay and the Canadian

353   Arctic Archipelago, highlighting the freshwater influx in these near-shore areas. In

354   contrast to our observations in Baffin Bay, DMS concentrations showed relatively little

355   variability across these salinity gradients.

356   In order to more closely examine small-scale variability in DMS and other surface

357   water variables, we calculated spatial gradients in the data to examine the coherence of

358   frontal features in DMS, salinity, temperature and chl *a* fluorescence. For this analysis,

359   we computed gradients in each oceanographic variable within a neighborhood of 100

360   points surrounding each point. Gradients (G) for each variable (DMS, SST, chl *a*, and

361   salinity) were calculated at each point x as follows:

$$G_x = \frac{V_{x+50} - V_{x-50}}{D_{x+50} - D_{x-50}}$$

362   (2)

363   Here, G is gradient (in units of change per km), V is the value of the variable at a

364   point, x, and D is the cruise track distance at x. A neighborhood of 100 points was

17

Biogeosciences
Discussions

Open Access

EGU

365   subjectively chosen because it best captured the observed variability in the data,

366   representing an intermediate value between a localized neighborhood (e.g. 10 points),

367   which would only consider changes close to the point, and a large neighborhood (e.g.

368   1000 points), which would smooth the features. The results of this analysis (Fig. 4)

369   qualitatively demonstrate a coherence of DMS gradients with salinity, chlorophyll, and

370   sea surface temperature.

371   **3.6 Correlation with ancillary oceanographic variables**

372   We computed Pearson correlation coefficients of DMS and DMSP with underway

373   measurements of salinity, sea surface temperature, chl a fluorescence, and sea ice cover.

374   We also examined the potential relationships between DMS concentrations and MIMS-

375   derived pCO$_2$, and ΔO$_2$/Ar (Tortell et al., in preparation). The results can be seen in Table

376   3. Only correlations significant at the 0.05 level are included. Only weak correlations are

377   seen between MIMS-measured DMS data and ancillary variables, and OSSCAR DMS

378   data did not exhibit any significant correlations with any ancillary variables, including

379   measured of phytoplankton taxonomic distributions. A strong positive correlation ($r =$

380   0.66, $p<0.001$) was found between DMSP and underway chl a fluorescence. Over the

381   whole transect, we observed a weak negative correlation between DMS/P and sea-ice

382   cover ($r = -0.26$ for DMS, and $r=-0.34$ for DMSP, $p< 0.001$ in both cases). A weak

383   positive correlation was found between DMSP/chl a and ice cover ($r = 0.52$, $p< 0.04$),

384   suggesting potential roles for sea-ice microalgae in DMSP production at the sampled

385   stations. It is interesting to note that elevated chl a fluorescence and DMSP

386   concentrations often occurred in areas of intermediate ice cover (km 3300, 7300 and 9200

18

387   along the cruise track), potentially reflecting the influence of ice-edge blooms or under-

388   ice phytoplankton assemblages. Potential mechanisms for these features are addressed in

389   the discussion.

390   **4. Discussion**

391   Our results provide a new dataset of reduced sulfur compounds in an under-

392   sampled region of the Arctic Ocean, and enable an examination of DMS/P variability in

393   relation to a number of oceanographic properties on a range of spatial scales. Below, we

394   focus our discussion on the observed relationship between gradients in DMS and other

395   oceanographic variables, and discuss the comparability of the two DMS measurement

396   methods utilized.   We compare our results to previously published measurements in the

397   Arctic, situating our results in the context of the changing hydrography and

398   phytoplankton ecology of the Arctic Ocean.

399   **4.1 Comparability of MIMS and OSSCAR measurements**

400   The OSSCAR and MIMS instruments have previously shown good agreement in

401   measured DMS concentrations in the Subarctic Pacific Ocean (Asher et al. 2015).

402   Similarly, we observed relatively good coherence between the two methods (Fig. 3) over

403   much of our cruise track. The largest exception to this occurred around km 7000, when

404   DMS measurements measured by OSSCAR were significantly higher than those

405   measured by MIMS. This region was characterized by very high DMSP measurements

406   (often one order of magnitude higher than the DMS measurements). If small amounts of

407   DMS remained in the OSSCAR system after DMSP analysis, sample carry-over could

408   contribute to higher measured concentrations in the subsequent DMS analysis. In order

19

409   to minimize this potential artifact, the system was thoroughly rinsed with MilliQ water

410   after every run. It is possible, however, that this approach was not entirely efficient.

411   Another potential cause of the higher OSSCAR DMS measurements may be due to cell

412   breakage during the sparging process in OSSCAR. In this scenario, there is the potential

413   for release of intracellular DMSP and DMSP lyase into solution, which would lead to

414   artificially high measured DMS concentrations. It is not possible for us to quantify the

415   magnitude of such a potential artefact, but we note that its magnitude would likely

416   depend on the taxonomic composition of phytoplankton assemblages. Wolfe et al (2002)

417   showed that sample sparging led to an increase in DMS production by both the

418   haptophyte *Emiliana huxleii* and the dinoflagellate *Alexandrium.* (Wolfe et al, 2002).

419   Unfortunately, due to limited coverage of discrete sampling, we do not have any

420   estimates of phytoplankton community composition in the region where MIMS and

421   OSSCAR showed the greatest discrepancies. Notwithstanding these potential caveats, we

422   suggest that the two methods show strong promise to provide complementary information

423   on DMS/P (and DMSO) concentrations in surface ocean waters.

424   One challenge going forward is to increase the reproducibility of OSSCAR

425   measurements, and this is an area of active work in our group. Moreover, we have

426   recently worked to significantly improve the limit of detection. The version of our

427   system used in 2015 had a detection limit of roughly 1.4 nM, and was thus far less

428   sensitive than many conventional GC methods, which can achieve sub-nM detection

429   limits. Our detection limit was of only minor consequence for DMSP measurements,

430   given that 72% of measured DMSP concentrations were higher than 10 nM, and less than

431   3% fell below 1.4 nM. The relatively low sensitivity was somewhat more problematic

432   for DMS, with approximately 22% of our OSSCAR-measured DMS values below 1.4

433   nM. Nonetheless, as discussed below, we believe that the OSSCAR data, in combination

434   with our MIMS data, provide useful information on the spatial distribution of both DMSP

435   and DMS in Arctic waters.

436   **4.2 Towards a regional Arctic data base of DMS/P concentrations**

437   Figure 6 shows a comparison between our Arctic DMS measurements (made by

438   OSSCAR) and other summertime Arctic DMS data in the PMEL database. For this

439   comparison, only PMEL measurements made above the Arctic circle (66.56° N) in June-

440   August were included, resulting in a total of 415 data points. As shown in Fig. 6, the

441   majority of available summertime PMEL DMS/P measurements are found in the Atlantic

442   region of the Arctic, and in the Bering Sea, with limited data in the Canadian Archipelago

443   (for an overview of Arctic DMS/P studies performed to date, see Levasseur, 2013). For

444   the sake of visual clarity, the presentation of data in Fig. 6a, is based on DMS

445   measurements made by OSSCAR, whereas both sets of data were included in the

446   frequency distribution analysis (Fig. 6b).The results presented in Fig. 6 suggest that our

447   measurements are representative of the broader Arctic context, with generally similar data

448   frequency distributions (Fig. 6b) for all three DMS datasets (MIMS, OSSCAR, and

449   PMEL). From the map, we see that the spatial footprint of our measurements complement

450   the existing summer data, helping to expand the spatial coverage of DMS observations in

451   the Arctic Ocean. While the PMEL data base does not include information needed to

452   directly calculate sea-air fluxes, the range of sea-air fluxes we calculated (~ 1 – 80 μmol

21

453   m^{-2} d^{-1}) was consistent with recent summertime sea-air DMS fluxes modeled in Resolute

454   Bay (Hakase Hayashida, pers. comm.).

455   In addition to complementing the existing PMEL DMS database, our new

456   observations also build on a number of other reduced sulfur measurements in the

457   Canadian Sector of the Arctic Ocean. Observations of DMS and DMSP derived from

458   several past Arctic and subarctic Atlantic surveys are summarized in Table 5. This table

459   focuses heavily on DMS and DMSP measurements made in the Canadian sector and

460   Greenland waters, serving to provide context for our measurements performed in similar

461   environments. The data presented in Table 5 are drawn from different times of year, and

462   from phytoplankton assemblages of varying taxonomic composition, allowing us to

463   examine sulfur accumulation in surface waters under a range of environmental and

464   ecological conditions.   For example, Bouillon et al. (2002) observed low DMS

465   concentrations (<1nM) during a large spring diatom bloom (~ 15 μg L^{-1}chl a) in the North

466   Water region. In contrast, higher DMS concentrations have been reported later in the

467   season when total phytoplankton biomass is lower, and taxonomic composition has

468   shifted away from diatom-dominance. Working in the same geographic region as

469   Bouillon, Motard-Côté et al. (2012) reported higher late summer (September) DMS

470   levels (maximum = 4.8nM), which were accompanied by moderate chl a concentrations

471   (0.2-1 μgL^{-1}), while Luce et al. (2011) reported very low DMS (<1nM) associated with

472   moderate chl a concentrations (0.2-2 μgL^{-1}) in a flagellate dominated community in late

473   fall (October-November), with DMS decreasing towards the later months. A similar

474   pattern was observed in the Northwest Subarctic Atlantic by Lizotte et al (2012), who

22

475   associated elevated reduced sulphur (DMSP) production with flagellate and

476   prymnesiophyte communities in midsummer and fall, in contrast to early-season diatom

477   blooms with little associated DMSP and DMS. This seasonal decrease in DMS levels

478   may be potentially attributable to light limited primary productivity, and diminishing

479   capacity for light-induced oxidative stress, which has been shown to increase DMS/P

480   production (Sunda et al., 2002).

481   To date, the highest recorded Arctic water column measurements of DMS (25nM)

482   and DMSP (160 nM) have been observed during mid-summer blooms of the haptophyte

483   *Phaeocystis* at the ice edge (see Matrai and Vernet, 1997; Gali and Simo, 2010). Our mid-

484   season (July-August) study of similar areas shows moderately high DMS (up to 18 nM)

485   accompanied by relatively low chl *a* (0.11- 1.06 μgL^{-1}) in a mixed community where

486   flagellates and prasinophytes are present (see discussion of HPLC pigments).

487   Together, the available data (Table 5 and our measurements) are consistent with a

488   seasonal cycle in Arctic and subarctic reduced sulfur distributions. Early season diatom-

489   dominated blooms exhibit high biomass and primary productivity but low DMS/P

490   accumulation, while mid-summer phytoplankton assemblages dominated by haptophytes

491   and dinoflagellates display lower phytoplankton biomass but higher reduced sulfur

492   accumulation. This pattern is similar to the summertime 'DMS paradox' in lower latitude

493   temperate and sub-tropical marine waters (Simo and Pedrós-Alió, 1999). In the fall, both

494   Arctic primary productivity and DMS/P production decrease with the onset of lower

495   temperatures and increased ice cover. Our data are consistent with this general scenario,

496   representing a mixed-species assemblage with moderate biomass and DMS/P

497   accumulation.

4.3 Gradients in DMS and hydrographic frontal structures

499   The high resolution afforded by the MIMS dataset allows for the observation of

500   fine-scale variability in DMS concentrations at the sub-kilometer scale. Previous studies

501   (Tortell, 2005; Tortell et al., 2011) have previously quantified fine-scale variability in

502   DMS concentrations, demonstrating de-correlation length scales on the order of 10s of

503   Km, and often shorter than that of other oceanographic variables such as temperature and

504   salinity. Figures 2 and 4 clearly demonstrate that gradients in DMS and chl *a*

505   fluorescence often co-occur with strong gradients in temperature and salinity. This

506   suggests a potential role for hydrographic fronts in driving changes in DMS

507   concentrations. Several potential mechanisms may explain this phenomenon. For

508   example, the frontal mixing of distinct water masses, driven by currents, wind, or melting

509   ice, may introduce nutrients into a low-nutrient water column, stimulating primary

510   productivity and potentially increasing DMS/P production. This stimulation of primary

511   productivity has been observed previously by other groups. For example, Tremblay et al.

512   (2011) showed that introduction of nutrient-rich water masses through ice ablation and

513   upwelling led to large (2-6 fold) increases in phytoplankton primary productivity

514   (Tremblay et al., 2011). Mixing of water masses may also potentially expose water

515   column phytoplankton to light shock or osmotic stress by mixing them upwards in the

516   water column or introducing an abrupt salinity gradient. Both of these factors could

517   contribute to elevated DMSP production, given its hypothesized role as an intracellular

24

518   osmolyte and anti-oxidant (Stefels et al., 2007). Though our data do not allow

519   mechanistic interpretation for the underlying causes of DMS variability in surface waters,

520   the high resolution afforded by MIMS measurements enables real-time observations of

521   DMS gradients, which may be useful in the design of future process studies examining

522   the driving forces for elevated DMS accumulation.

523   Fully resolving the production and consumption dynamics of DMS/P in seawater

524   requires a series of time-consuming and laborious methods, including various isotope

525   tracer studies and quantification of multiple physical process rates (e.g. photo-oxidation).

526   Clearly, it is not possible to conduct such measurements with the high frequency of our

527   MIMS-based DMS measurements. However, use of real-time MIMS monitoring will

528   enable the selection of targeted sampling locations to best leverage sampling efforts. In

529   this respect, the recent work of Asher et al. (2016) provides some example of how high

530   resolution DMS/P measurements can be coupled with isotope tracer studies to derive

531   insight into DMS/P dynamics in high latitude marine waters.

532   **4.4 Phytoplankton assemblage composition and mixed layer depth**

533   The majority of the sampled stations were characterized by very shallow mixed

534   layer depths (MLD; Table 2) resulting from strong salinity-based stratification of surface

535   waters. Light stress associated with shallow MLD may contribute to elevated DMSP : chl

536   *a* ratios. In our dataset, the shallowest MLDs were observed at stations BB3 and CAA6

537   (8.2 m and 6.1 m, respectively), and these stations were also characterized by elevated

538   DMSP concentrations. The elevated DMSP : chl *a* ratios measured in our study also

539   reflect the presence of high-DMSP producing taxa, a phenomenon also reported by other

25

Biogeosciences

Discussions

Open Access

EGU

540   groups (Matrai et al. 1997; Gali et al., 2010; Lizotte et al., 2012). Limited HPLC station

541   data suggest that a mixed phytoplankton assemblage was present in the study area at the

542   time of sampling. When comparing our DMSP: chl a ratios to other measurements, it is

543   important to note that we measured $DMSP_t$, while many other groups present results in

544   terms of $DMSP_p$, without taking into account the dissolved fraction ($DMSP_d$). As the

545   dissolved DMSP pool typically makes up a small (though highly variable) portion of the

546   total water column DMSP pool, the use of DMSPt does not likely have a large effect on

547   derived DMSP:chl a ratios (Kiene et al., 2000; 2006). Moreover, we used HPLC-derived

548   chl a for these calculations, as opposed to the more standard fluorometric chl a

549   measurements. HPLC chl a measurements are likely to be more accurate than

550   fluorometric measurements, and tend to yield lower concentrations, acting to increase

551   DMSPt:chl a (Welschmeyer 1994) .

552   Despite the potential caveats raised above, the $DMSP_t$:chl a ratios we measured

553   across our sampling stations (52-182 nMµg^{-1}) were broadly similar to $DMSP_p$:chl a

554   values found by Motard-Côté et al. (15-229 nMµg^{-1}) in the same region in September

555   (Motard-Côté et al., 2011). In contrast, our measured $DMSP_t$:chl a ratios are significantly

556   higher than those measured by Luce et al. (maximum of 39 nMµg^{-1}) (Luce et al., 2007)

557   and Matrai and Vernet (maximum 17 nmol µg^{-1}) at diatom-dominated stations in the

558   Barents Sea (Matrai and Vernet., 1997). This difference likely reflects a difference in

559   phytoplankton assemblage composition, even though we were unable to find any

560   significant correlations between DMSP:Chl and HPLC pigment markers for different

561   phytoplankton groups. It may be that the taxonomic composition of our sampled

562 assemblages was not sufficiently variable to enable large differences in DMSP:chla

563 values.

4.5 The interaction of DMS/P and sea ice

565 The presence of sea ice exerts a strong control on polar phytoplankton by limiting

566 irradiance for primary productivity in the water column. This allows high concentrations

567 of nutrients to accumulate, creating favorable conditions for phytoplankton blooms upon

568 sea-ice melt. Ice edge blooms are well documented, and can serve as a source for

569 reduced sulfur compounds. In a 2010 study, Gali et al found that sea ice melt drove

570 stratification of nutrient rich surface water, triggering a sharp increase in primary

571 productivity, with associated elevated DMS and DMSP levels (Gali et al., 2010). A

572 number of recent studies have also examined the potential of sea ice to act as a reservoir

573 of reduced sulfur. For example, Levasseur et al (1994) reported very high concentrations

574 of DMS and DMSP in Arctic bottom-ice diatoms, and suggested that the breakup of sea

575 ice may stimulate reduced sulfur production by triggering phytoplankton blooms and

576 releasing accumulated sulfur into the water column. In a more recent study , Galindo et al

577 (2016) demonstrated experimentally that the exposure of phytoplankton to high light

578 conditions (mimicking those that would follow the breakup of sea ice) led to near-total

579 release of intracellular DMSP, providing one possible explanation for elevated DMSP

580 levels in the water column.

581 The weak negative correlations between sea ice cover and DMS/P concentration

582 we observed is consistent with the idea that sea ice cover limits insolation, thereby

583 reducing primary productivity and DMS/P production. In general, the drivers of DMSP

27

584   and DMS production differ – though DMSP production has been shown to be directly

585   influenced by sea ice melt in under-ice blooms [30a], the production of DMS from DMSP

586   is largely dependent on the metabolism of in situ bacterial assemblages (Zubkov et al,

587   2001), and may therefore be uncoupled from the influence of ice on phytoplankton

588   activity. It is interesting to note, however, that several sharp increases in DMS occurred

589   simultaneously with the occurrence of small amounts of sea ice (<20% total cover) (Fig.

590   2, kms 3400 and 7200 on the cruise track). Limited station data also indicate high

591   DMS/P:chl a ratios in areas with a comparatively high sea ice cover, at stations BB3 and

592   CAA6 (Table 2). At the time of our sampling, both of these stations were characterized

593   by very low phytoplankton biomass (0.11 μgL^{-1} and 0.20 μg L^{-1}chl a, respectively) and

594   had particularly high DMSP: chl a ratios (129 nmol μg^{-1} and 182 nmol μg^{-1},

595   respectively). This suggests a potential role for ice-edge effects, either through the melt-

596   induced stimulation of reduced sulfur production in DMS/P rich phytoplankton taxa, or

597   through the release of ice-associated DMS/P into the water column. Figures 2d and 2e

598   show decreased salinity in partially ice-covered areas, in particular around kms 4400,

599   7300, and 9200. Similar trends have been reported by several groups. For instance,

600   Matrai and Vernet (1997) reported significantly higher values of DMS and DMSP in

601   partially ice-covered waters of the Barents Sea relative to ice-free regions, while Gali et

602   al. (Gali et al., 2010) and Leck and Persson (1997) reported highest DMS/P values along

603   the ice edge in their Arctic surveys.

604   **4.6 DMS in a changing Arctic**

605   The Arctic marine ecosystem is currently undergoing a dramatic warming that is

606   expected to have far-reaching impact on phytoplankton dynamics and, likely, DMS

607   production and sea-air fluxes. Much of the ecosystem change is driven by warming and

608   rapidly melting sea ice, which influences mixed layer stratification, light regimes and

609   nutrient supply. Current work suggests that sea ice loss will eventually lead to a nutrient-

610   poor, shallow-stratified Arctic Ocean with low phytoplankton biomass (Levasseur, 2013).

611   Nutrient limitation may favor smaller cells, shifting diatom-dominated assemblages to

612   communities with a strong flagellate presence, and this may, in turn, increase DMSP

613   production and DMS emissions. A modeling study by Gabric et al (2005) projected

614   significant increases in DMS emissions in response to MLD shoaling and ice ablation.

615   Our observations from regions with shallow mixed layer depths and mixed phytoplankton

616   assemblages do indeed exhibit elevated DMSP:chl ratios, providing some support for

617   this prediction.   On-going monitoring work will be needed to examine climate-driven

618   shifts in surface water productivity and biogeochemical cycles in Arctic Ocean waters.

619   **5. Conclusion**

620   We present a high spatial resolution dataset of reduced sulfur measurements

621   through the Canadian sector of the Arctic Ocean and Subarctic Atlantic. We demonstrate

622   the utility of high-resolution DMS measurements for comparison with other

623   oceanographic variables, and show the coherence of DMS gradients with fine-scale

624   surface hydrographic structure, suggesting elevated DMS production in some

625   oceanographic frontal zones. We also observed elevated DMS/P values in partially ice-

626   covered regions, suggesting that ice-edge effects may stimulate DMS/P production. Our

29

627   data serve to significantly expand the existing spatial coverage of reduced sulfur

628   measurements in the Arctic, providing a baseline for future studies in this rapidly

629   changing marine environment. Future warming of surface waters and sea-ice melt could

630   lead to increased concentrations and sea-air fluxes of DMS, though significantly more

631   observations will be needed to substantiate this.

632   **Acknowledgements:** This work was supported by grants from the Natural Sciences and

633   Engineering Research Council of Canada (NSERC) through the Climate Change and

634   Atmospheric Research program (Arctic-GEOTRACES). We are grateful to the captain

635   and crew of the *CCGS Amundsen* for their invaluable support in this work.

636

637   **Data Availability:**

638   All data are available at the following github repository:

639   **https://github.com/tjarnikova/Jarnikova_Canadian_Arctic_DMS_supldata** **(DOI:**

640   **10.5281/zenodo.160225**)

References

Arrigo, K.R., van Dijken, G., and Pabi, S.: Impact of a shrinking Arctic ice cover on
    marine primary production, Geophys. Res. Lett., 35, L19603,
    doi:10.1029/2008GL035028, 2008.

Arrigo, K.R., Perovich, D.K., Pickart, R.S., and Brown, Z.W.: Massive phytoplankton
    blooms under Arctic sea ice, Science, 336,1408, doi:10.1126/science.1215065,
    2012.

Asher, E., Dacey, J., Jarníková, T., and Tortell, P.: Measurement of DMS, DMSO, and
    DMSP in natural waters by automated sequential chemical analysis, Limnol.
    Oceanogr-Meth., 13, 451–462, doi:10.1002/lom3.10039, 2015.

Asher, E., Dacey, J., Stukel, M., Long, M.C., and Tortell, P.: Processes driving seasonal
    variability in DMS, DMSP, and DMSO concentrations and turnover in coastal
    Antarctic waters, Limnol. Oceanogr., 62, 104-124, doi: 10.1002/lno.10379, 2016.

Bouillon, R.C., Lee, P.A., de Mora, S.J., and Levasseur., M.: Vernal distribution of
    dimethylsulphide, dimethylsulphoniopropionate, and dimethylsulphoxide in the
    North Water in 1998, Deep-Sea Res., 49, 5171-5189, doi:10.1016/S0967-
    0645(02)00184-4, 2002.

Boyd, P.W., Crossley, A.C., DiTullio, G.R., Griffiths, F.B., Hutchins, D.A., Queguiner,
    B., Sedwick, P.N. and Trull, T.W.: Control of phytoplankton growth by iron supply
    and irradiance in the subantarctic Southern Ocean: Experimental results from the

666   SAZ Project, J. Geophys. Res., 106, 31573–31583, doi:10.1029/2000JC000348,

667   2001.

668

669   Carmack, E., and McLaughlin, F.: Towards a recognition of physical and geochemical

670   change in Subarctic and Arctic Seas, Prog. Oceanogr., 90, 90-104, doi:

671   10.1016/j.pocean.2011.02.007, 2011.

672

673   Carr, M.-E., Friedrichs, M.A.M, Schmeltz, M., Aita, M.N., Antoine, D., Arrigo, K.R.,

674   Asanuma, I., Aumont, O., Barber, R., Behrenfeld, M. Bidigare, R., Buitenhuis,

675   E.T., Campbell, J., Ciotti, A., Dierssen, H., Dowell, M., Dunne, J., Esaias, W.,

676   Gentili, B., Gregg, W., Groom, S., Hoepffner, N., Ishizaka, J., Kameda, T., Le

677   Quéré, C., Lohrenz, S., Mara, J., Mélin, F., Moore, K., Morel, A., Reddy, T., Ryan,

678   J., Scardi, M., Smyth, T., Turpie, K., Tilstone, G., Waters, K., and Yamanaka, Y.: A

679   comparison of global estimates of marine primary production from ocean color,

680   Deep-Sea Res. Pt. II., 53, 741–770, doi:10.1016/j.dsr2.2006.01.028, 2006.

681

682   Cavelieri, D.J., Markus, T., Hall, D. K., Gasiewski, A. J., Klein, M., and Ivanoff, A.:

683   Assessment of EOS Aqua AMSR-E Arctic Sea Ice Concentrations Using Landsat-7

684   and Airborne Microwave Imagery, IEEE T. Geosci. Remote., 44, 3057-3069, doi:

685   10.1109/TGRS.2006.878445, 2006.

686

687   Chang, R., Sjostedt, S., Pierce, J., Papakyriakou, T., Scarratt, M., Michaud, S.,

688   Levasseur, M., Leaitch, R., and Abbatt, J.: Relating atmospheric and oceanic DMS

689   levels to particle nucleation events in the Canadian Arctic, J. Geophys. Res., 116,

690   D00S03, doi:10.1029/2011JD015926, 2011.

691

692   Charlson, R., Lovelock, J., Andreae, M., and Warren, S.: Oceanic phytoplankton,

693   atmospheric sulphur, cloud albedo and climate, Nature, 326, 655–661,

694   doi:10.1038/326655a0, 1987.

695

696   Coupel, P., Matsuoka, A., Ruiz-Pino, D., Gosselin, M., Marie, D., Tremblay, J.-É., and

697   Babin, M.: Pigment signatures of phytoplankton communities in the Beaufort Sea,

698   Biogeosciences, 12, 991–1006, doi:10.5194/bg-12-991-2015, 2015.

699

700   Dacey, J., and Blough, N.V.: Hydroxide decomposition of dimethylsulfoniopropionate to

701   form dimethylsulfide, Geophys. Res. Lett., 14, 1246-1249,

702   doi:10.1029/GL014i012p01246, 1987.

703

704   DiTullio, G., Grebmeier, J., Arrigo, K., Lizotte, M., Robinson, D., Leventer, A., Barry, J.,

705   VanWoert, M., and Dunbar, R.: Rapid and early export of Phaeocystis antarctica

706   blooms in the Ross Sea, Antarctica, Nature, 404, 595–598, doi:10.1038/35007061,

707   2000.

708

709   Gabric, A., Simó, R., Cropp, R., Hirst, A., and Dachs, J.: Modeling estimates of the

710   global emission of dimethylsulfide under enhanced greenhouse conditions, Global

711   Biogeochem. Cy., 18, GB2014, doi:10.1029/2003GB002183, 2004.

712

713   Galí, M, and Simó, R.: Occurrence and cycling of dimethylated sulfur compounds in the

714   Arctic during summer receding of the ice edge, Mar. Chem., 122, 105-117,

715   doi:10.1016/j.marchem.2010.07.003, 2010.

716

Biogeosciences
Discussions

EGU

Open Access

717   Galindo, V., Levasseur, M., Mundy, C.J., Gosselin, M., Tremblay, J. -É., Scarratt, M.,

718   Gratton, Y., Papakiriakou, T., Poulin, M., and Lizotte, M.: Biological and physical

719   processes influencing sea ice, under‐ice algae, and dimethylsulfoniopropionate

720   during spring in the Canadian Arctic Archipelago, J. Geophys. Res-Oceans, 119,

721   3746–3766, doi:10.1002/2013jc00949, 2014.

722

723   Galindo, V., Levasseur, M., Mundy, C.J., Gosselin, M., Scarratt, M., Papakyriakou, T.,

724   Stefels, J., Gale, M., Tremblay, J.-É., and Lizotte, M.: Contrasted sensitivity of

725   DMSP production to high light exposure in two Arctic under-ice blooms, J. Exp.

726   Mar. Biol. Ecol., 475, 38–48, doi:10.1016/j.jembe.2015.11.009, 2016.

727

728   Keller, M.D.: Dimethyl sulfide production and marine phytoplankton: the importance of

729   species composition and cell size, Biological Oceanography, 6, 375-382,

730   doi:10.1080/01965581.1988.10749540, 1989.

731

732   Kiene, R., Linn, L. J., and Bruton, J.A.: New and important roles for DMSP in marine

733   microbial communities, J. Sea Res., 43, 209-224, doi: 10.1016/S1385-

734   1101(00)00023-X, 2000.

735

736   Kiene, R.P., and Linn, L.J.: Distribution and turnover of dissolved DMSP and its

737   relationship with bacterial production and dimethylsulfide in the Gulf of Mexico,

738   Limnol. Oceanogr., 45, 849-861, doi:10.4319/lo.2000.45.4.0849, 2000.

739

740   Kiene, R., and Slezak, D.: Low dissolved DMSP concentrations in seawater revealed by

741   small‐volume gravity filtration and dialysis sampling, Limnol. Oceanogr.-Meth., 4,

742   80–95, doi:10.4319/lom.2006.4.80, 2006.

34

Biogeosciences

Discussions

Open Access

EGU

743

744   Lana, A., Bell, T.G., Simó, R., Vallina, S.M., Ballabrera-Poy, J., Kettle, A.J., Dachs, J.,

745   Bopp, L., Saltzman, E.S., Stefels, J., Johnson, J.E., and Liss, P.S.: An updated

746   climatology of surface dimethlysulfide concentrations and emission fluxes in the

747   global ocean, Global Biogeochem. Cy., 25, GB1004, doi:10.1029/2010GB003850,

748   2011.

749

750   Leck, C., and Persson, C.: The central Arctic Ocean as a source of dimethyl sulfide

751   Seasonal variability in relation to biological activity, Tellus B, 48B(2), 156–177,

752   doi:10.1034/j.1600-0889.1996.t01-1-00003.x, 1996.

753

754   Levasseur, M., Gosselin, M., and Michaud, S.: A new source of dimethylsulfide (DMS)

755   for the arctic atmosphere: ice diatoms, Mar. Biol., 121, 381–387,

756   doi:10.1007/BF00346748, 1994.

757

758   Levasseur, M., Impact of Arctic meltdown on the microbial cycling of sulphur, Nat.

759   Geosci., 6, 691–700, doi:10.1038/ngeo1910, 2013.

760

761   Lizotte, M., Levasseur, M., Michaud, S., Scarratt, M., Merzouk, A., Gosselin, M.,

762   Pommier, J., Rivkin, R., and Kiene, R.: Macroscale patterns of the biological

763   cycling of dimethylsulfoniopropionate (DMSP) and dimethylsulfide (DMS) in the

764   Northwest Atlantic, Biogeochemistry, 110, 183–200, doi:10.1007/s10533-011-

765   9698-4, 2012.

766

767   Loose, B., McGillis, W.R., and Schlosser, P.: Effects of freezing, growth, and ice cover on

768   gas transport processes in laboratory seawater experiments, Geophys. Res. Lett.,

769   36, L05603, doi:10.1029/2008GL036318, 2009.

770

771   Luce, M., Levasseur, M., Scarrat, M.G., Michaud, S., Royer, S.-J., Kiene, R., Lovejoy,

772   C., Gosselin, M., Poulin, M., Gratton, Y., and Lizotte, M.: Distribution and microbial

773   metabolism of dimethylsulfoniopropionate and dimethylsulfide during the 2007

774   Arctic ice minimum, J. Geophys. Res.-Oceans, 116, C00G06,

775   doi:10.1029/2010JC006914, 2011.

776

777   Malin, G., Wilson, W.H., Bratbak, G., Liss, P.S., and Mann, N.H.: Elevated production of

778   dimethylsulfide resulting from viral infection of cultures of Phaeocystis pouchetii,

779   Limnol. Oceanogr., 43, 1389–1393, doi: 10.1016/S0967-0645(02)00184-4, 1998.

780

781   Martin, J., Tremblay, J. Gagnon, J., Tremblay, G., Lapoussière, A., Jose, C., Poulin, M.,

782   Gosselin, M., Gratton, Y., and Michel, C.: Prevalence, structure and properties of

783   subsurface chlorophyll maxima in Canadian Arctic waters, Mar. Ecol. Prog. Ser.,

784   412, 69–84, doi:10.3354/meps08666, 2010.

785

786   Matrai, P., and Vernet, M.: Dynamics of the vernal bloom in the marginal ice zone of the

787   Barents Sea: Dimethyl sulfide and dimethylsulfoniopropionate budgets, J. Geophys.

788   Res.-Oceans, 102, 22965-22929, doi:10.1029/96JC03870, 1997.

789

790   Michel, C., Ingram, R. G., and Harris, L. R.: Variability in oceanographic and ecological

791   processes in the Canadian Arctic Archipelago, Prog. Oceanogr., 71, 379–401,

792   doi:10.1016/j.pocean.2006.09.006, 2006.

36

793

794   Motard‑Côté, J., Levasseur, M., Scarratt, M.G., Michaud, S., Gratton, Y., Rivkin, R.B.,

795   Keats, K., Gosselin, M., Tremblay, J.-É., and Kiene, R.P.: Distribution and

796   metabolism of dimethylsulfoniopropionate (DMSP) and phylogenetic affiliation of

797   DMSP‑assimilating bacteria in northern Baffin Bay/Lancaster Sound, J. Geophys.

798   Res-Oceans, 117, C00G11, doi:10.1029/2011JC007330, 2012.

799

800   Mungall, E., Croft, B., Lizotte, M., Thomas, J., Murphy, J., Levasseur, M., Martin, R.,

801   Wentzell, J., Liggio, J., and Abbatt, J.: Dimethyl sulfide in the summertime Arctic

802   atmosphere: measurements and source sensitivity simulations, Atmospheric

803   Chemistry and Physics, 16, 6665–6680, doi:10.5194/acp-16-6665-2016, 2016.

804

805   Nightingale, P.D., Malin, G., and Law, C.S.: In situ evaluation of air‑sea gas exchange

806   parameterizations using novel conservative and volatile tracers, Global

807   Biogeochem. Cy., 14, 373-387, doi:10.1029/1999GB900091, 2000.

808

809   Pinckney, J., Papa, R., and Zingmark, R.: Comparison of high-performance liquid

810   chromatographic, spectrophotometric, and fluorometric methods for determining

811   chlorophyll a concentrations in estaurine sediments, Journal of Microbiol. Meth.,

812   19, 59–66, doi:10.1016/0167-7012(94)90026-4, 1994.

813

814   Saltzman, E.S., King, D.B., Holmen, K., and Leck, C.: Experimental determination of the

815   diffusion coefficient of dimethylsulfide in water, J. Geophys. Res., 98, 16481–

816   16486, doi:10.1029/93JC01858, 1993.

817

818   Scarratt, M., Levasseur, M., Michaud, S., and Roy, S.: DMSP and DMS in the Northwest

819   Atlantic: Late-summer distributions, production rates and sea-air fluxes, Aquat.

820   Sci., 69, 292–304, doi:10.1007/s00027-007-0886-1, 2007.

821

822   Simó, R., and Pedrós-Alió, C.: Role of vertical mixing in controlling the oceanic

823   production of dimethyl sulphide, Nature, 402, 396–399, doi:10.1038/46516, 1999.

824

825   Simó, R.: Production of atmospheric sulfur by oceanic plankton: Biogeochemical,

826   ecological and evolutionary links, *Trends Ecol. Evol.*, **16**, 287–294,

827   doi:10.1016/S0169-5347(01)02152-8, 2001.

828

829   Smith, W., Marra, J., Hiscock, M., and Barber, R.: The seasonal cycle of phytoplankton

830   biomass and primary productivity in the Ross Sea, Antarctica, Deep-Sea Res. Pt.

831   II., 47, 3119–3140, doi:10.1016/S0967-0645(00)00061-8, 2000.

832

833   Stefels, J., Steinke, M., Turner, S., Malin, G., and Belviso, S.: Environmental constraints

834   on the production and removal of the climatically active gas dimethylsulphide

835   (DMS) and implications for ecosystem modelling, Biogeochemistry, 83, 245–275,

836   doi:10.1007/s10533-007-9091-5, 2007.

837

838   Sunda, W., Kieber, D.J., Kiene, R.P., and Huntsman, S.: An antioxidant function for

839   DMSP and DMS in marine algae, Nature, 418, 317–20, doi:10.1038/nature00851,

840   2002.

841

842   Taylor, R. L., Semeniuk, D. M., Payne, C. D., Zhou, J., Tremblay, J., Cullen, J. T., and

843   Maldonado, M. T.: Colimitation by light, nitrate, and iron in the Beaufort Sea in

844   late summer, J. Geophys. Res.-Oceans, 118, 3260–3277, doi:10.1002/jgrc.20244.,

845   2013.

846

847   Tortell, P.D., Dissolved gas measurements in oceanic waters made by membrane inlet

848   mass spectrometry, Limnol. Oceanogr.-Meth., 3, 24-37, doi:

849   10.4319/lom.2005.3.24, 2005.

850

851   Tortell, P. D., Guéguen, C., Long, M. C., Payne, C. D., Lee, P., and DiTullio, G. R.:

852   Spatial variability and temporal dynamics of surface water pCO2, ΔO2/Ar and

853   dimethylsulfide in the Ross Sea, Antarctica, Deep-Sea Res. Pt. I., 58, 241–259,

854   doi:10.1016/j.dsr.2010.12.006, 2011.

855

856   Tremblay, J.E., Michel, C., Hobson, K.A., Gosselin, M., and Price, N.: Bloom dynamics

857   in early opening waters of the Arctic Ocean, Limnol. Oceanogr. 51, pp.900-912.

858   doi: 10.4319/lo.2006.51.2.0900, 2006.

859

860   Tremblay, J., Bélanger, S., and Barber, D.G.: Climate forcing multiplies biological

861   productivity in the coastal Arctic Ocean, Geophys. Res. Lett., 38,

862   doi:10.1029/2011GL048825, 2011.

863

864   Welschmeyer, N.A., Fluorometric analysis of chlorophyll a in the presence of chlorophyll

865   b and pheopigments, Limnol. Oceanogr., 39, 1985-1992,

866   doi:10.4319/lo.1994.39.8.1985, 1994.

867

868   Wolfe, G.V., Strom, S.L., Holmes, J.L., Radzio, T. and Olson, M.B.:

869   Dimethylsulfoniopropionate cleavage by marine phytoplankton in response to

870   mechanical, chemical, or dark stress. Journal of Phycology, 38, 948-960.

871   doi:10.1046/j.1529-8817.2002.t01-1-01100.x, 2002.

872

873   Woodhouse, M.T, Carslaw, K.S., Mann, G.W., Vallina, S.M., Vogt, M., Halloran, P.R.,

874   and Boucher, O.: Low sensitivity of cloud condensation nuclei to changes in the

875   sea-air flux of dimethyl-sulphide, Atmospheric Chemistry and Physics, 10, 7545–

876   7559, doi:10.5194/acp-10-7545-2010, 2010.

877

878   Zubkov, M.V, Fuchs, B., Archer, S., Kiene, R., Amann, R., and Burkill, P.: Linking the

879   composition of bacterioplankton to rapid turnover of dissolved

880   dimethylsulphoniopropionate in an algal bloom in the North Sea, Environ.

881   Microbiol., 3, 304–311, doi:10.1046/j.1462-2920.2001.00196.x, 2001.

882

Biogeosciences
Open Access
Discussions
EGU

883   **Tables:**

Pigment	Associated Taxa
Chlorophyll c$_3$	Haptophytes
Peridinin	Dinoflagellates
19'-butanoyloxyfucoxanthin	Haptophyte
Fucoxanthin	Diatoms, Haptophytes
19'-hexanoyloxyfucoxanthin	Haptophytes, Dinoflagellates
Diadinoxanthin	Haptophytes, Dinoflagellates, Diatoms
Violaxanthin	Dinoflagellates
Zeaxanthin	Dinoflagellates

884

885   **Table 1.** HPLC marker pigments and their associated phytoplankton taxa. Adapted from

886   (Coupel et al. 2015) .

887

888

889

890

891

892

893

894

895

Station	Lat(N)	Lon(E)	MLD(m)	% Ice Cover	chla (ug L^{-1})	DMS/chla (nmol µg^{-1})	DMSP/chla (nmol µg^{-1})	Perid/chla	19'ButFuc/chla	Fuc/chla	19'HexFuc/chla	Diadino/chla
K1	56.12	-53.37	18.4	nd	0.51	6.6	nd	0.043	0.077	0.184	0.156	0.056
LS2	60.45	-56.55	41.4	nd	0.59	3.4	nd	0.051	0.012	0.277	0.025	0.024
BB3	71.41	-68.59	8.2	19.7	0.12	bdl	129.4	0.049	0.011	0.278	0.051	0.087
BB2	72.75	-67.00	10.3	nd	0.19	21.7	93.3	0.050	0.015	0.312	0.089	0.072
CAA1	74.52	-80.56	32.1	nd	0.56	6.9	52.3	0.015	0.018	0.239	0.023	0.042
CAA5	74.12	-91.49	5.3	6.61	0.16	bdl	114.7	0.078	0.017	0.326	0.020	0.051
CAA6	74.75	-97.47	6.1	16.43	0.21	10.6	181.7	0.054	0.021	0.401	0.015	0.058
CAA7	73.66	-96.53	2.1	13.3	0.13	15.6	81.3	0.109	0.066	0.335	0.057	0.146
VS	69.16	-100.69	8.4	8.23	0.18	10.6	nd	0.029	0.020	0.309	0.032	0.037

Table 2. Mixed layer depth (MLD), ice cover, HPLC pigment measurements (ratios of selected marker pigments to chl a), DMS (MIMS) and DMSP (OSSCAR) measurements. Perid = peridinin, 19'ButFuc = 19'-butanoyloxyfucoxanthin, Fuc = Fucoxanthin, 19'HexFuc = 19'-hexanoyloxyfucoxanthin, Diadino = Diadinoxanthin *nd*= no data. *bdl* = below detection limit.

918

Variable	DMS Correlation Coefficient	DMSP Correlation Coefficient
$\Delta O_2/Ar$	0.22	0.33
Salinity	0.35	0.34
SST	0.29	0.14
Fluorescence	0.32	0.66
pCO_2	0.16	0.12
Ice Cover	-0.26	-0.34

919

920 **Table 3** Pearson correlation coefficients relating DMS measurements made by MIMS and

921 DMSP measurements made by OSSCAR to other oceanographic variables. Only

922 correlations significant at the $p < 0.05$ level are shown. $\Delta O_2/Ar$ ratios were obtained using

923 MIMS.

924

925

926

927

928

929

930

931

932

933

43

Station	Diatom	Dinoflag.	Chloro.	Prasino	Crypto.	C-P	c3-Flag.	Hapto-7
K1	37	14	0	17	4	9	1	16
LS2	39	19	0	23	1	3	7	8
BB3	48	15	4	14	8	1	5	5
BB2	44	16	11	14	4	2	1	8
CAA1	47	4	0	39	2	2	4	2
CAA5	50	19	1	10	3	2	14	1
CAA6	52	16	1	8	3	2	17	1
CAA7	46	11	4	17	8	8	0	5
VS	67	8	0	11	3	3	6	3

934

935 **Table 4** CHEMTAX-derived phytoplankton assemblage estimates (numbers given are

936 percent of total chl a) for sampled stations. Diat. = diatoms; Dinoflag = Dinoflagellates;

937 Chloro. = Chlorophytes; Prasino = Prasinophyte (types 2 and 3); Crypto. = Cryptophytes

938 Chryso-Pelago =Chrysophytes/Pelagophytes; c3-flag. = c3-Flagellates; Hapto-7 =

939 Haptophyte type 7. Due to the presence of unidentified phytoplankton taxa, not all

940 assemblage estimates sum to 100%.

941

942

943

944

945

946

947

948

949

950

Author	Year	Month	Region	DMS (nM)	DMSP (nM)	Assemblage characteristics
Bouillon et al. (2002)	1998	April-June	North Water	0.04-6.7	0.9-53	Diatom dominated assemblage
Matrai et al. (1997)	1993	May	Barents Sea	2.8 - 25.3	6-27	Diatom-dominated and *Phaeocystis*-dominated stations
Lizotte et al. (2012)	2003	May-October	Northwest Atlantic	0.1-12	4-101	Nanoflagellate dominated in all seasons
Gali et al. (2010)	2007	July	Greenland Sea	0.1 - 18.3	1.4 - 163.6	Haptophyte (*Phaeocystis*) dominance
Leck et al. (1996)	1991	August-October	Greenland Sea	0.04 - 12	--	Not described
Motard-Côté et al. (2012)	2008	September	Baffin Bay North Water	0.4-5.2	5-70	
Scarratt et al. (2007)	1999	September	Northwest Atlantic	0.2-4.7	0-203	Mixed assemblage
Luce et al. (2011)	2007	October-November	High Arctic	0.05-0.8	2-39	Flagellate-dominated except for diatom-dominated in Baffin Bay
This study	2015	July-August	Canadian Arctic Archipelago	0.1-18	<1 - 160	Mixed assemblage, diatom-dominated

Table 5. Compilation of published Arctic and Subarctic Atlantic DMS/P data from the summer and fall months, focusing on observations from the Western Hemisphere.

971 **Figures:**
972
973
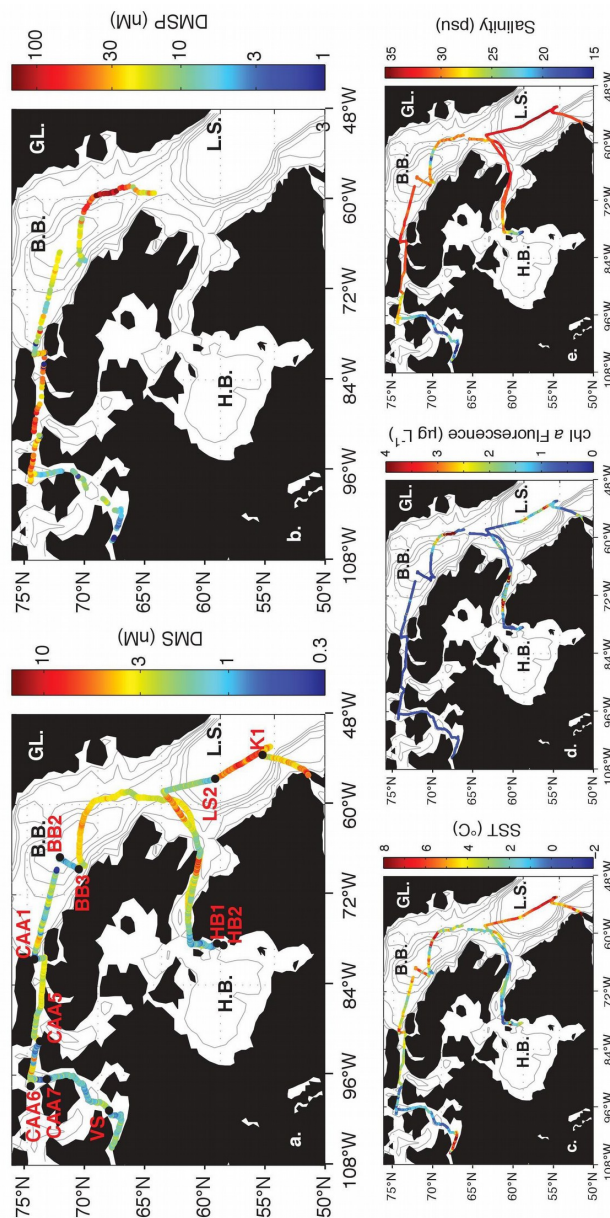
993 **Figure 1.** Spatial distribution of DMS, DMSP and hydrographic variables. GD. =

994 Greenland, B.B. = Baffin Bay, L.S = Labrador Sea, H.B. = Hudson Bay.
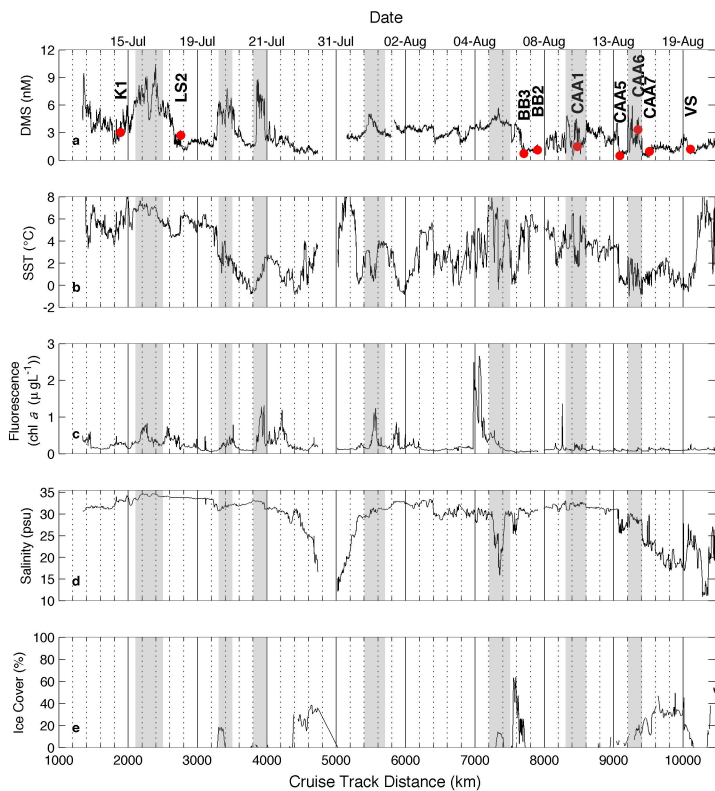
Figure 2. Distribution of DMS and hydrographic variables along our cruise track. Grey

shaded areas show denote regions of sharp increases in DMS.

998

999

1000

1001

1002

1003

1004

1005

1006

1007

1008

1009
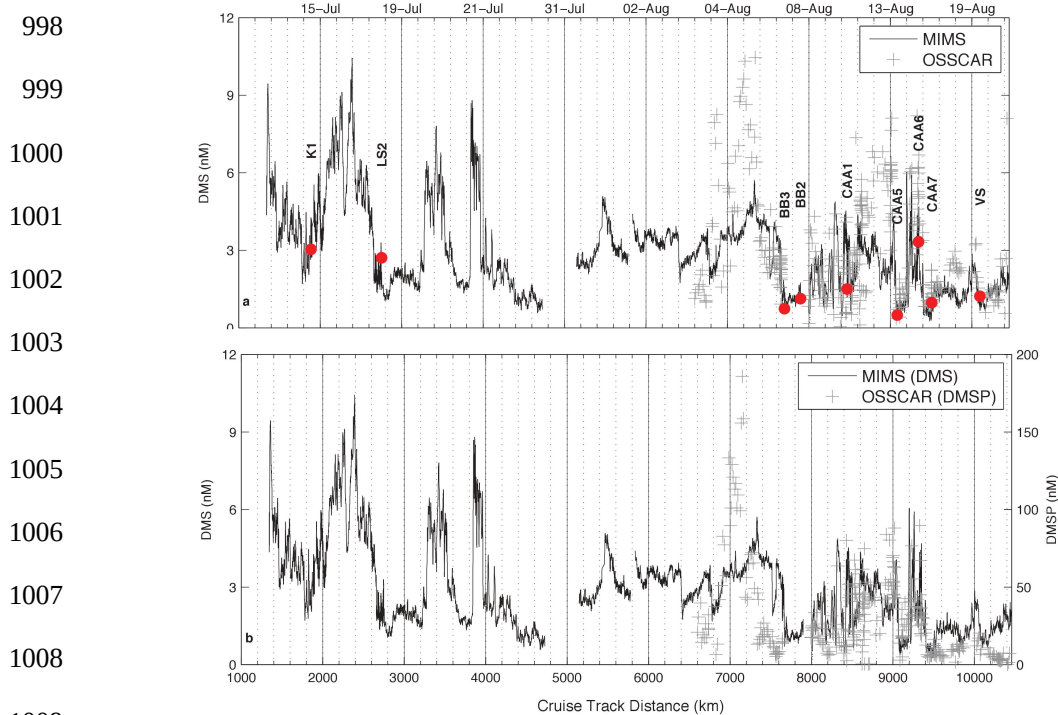
1010 **Figure 3.** Distribution of DMS and DMSP along the cruise track. Panel (a) shows DMS

1011 measurements made by MIMS and OSSCAR. Note that a small fraction (less than

1012 0.5%) of measurements made by OSSCAR were above 12 nM. Panel (b) shows MIMS

1013 data with OSSCAR DMSP measurements superimposed on a different y scale (right hand

1014 side).

1015

48
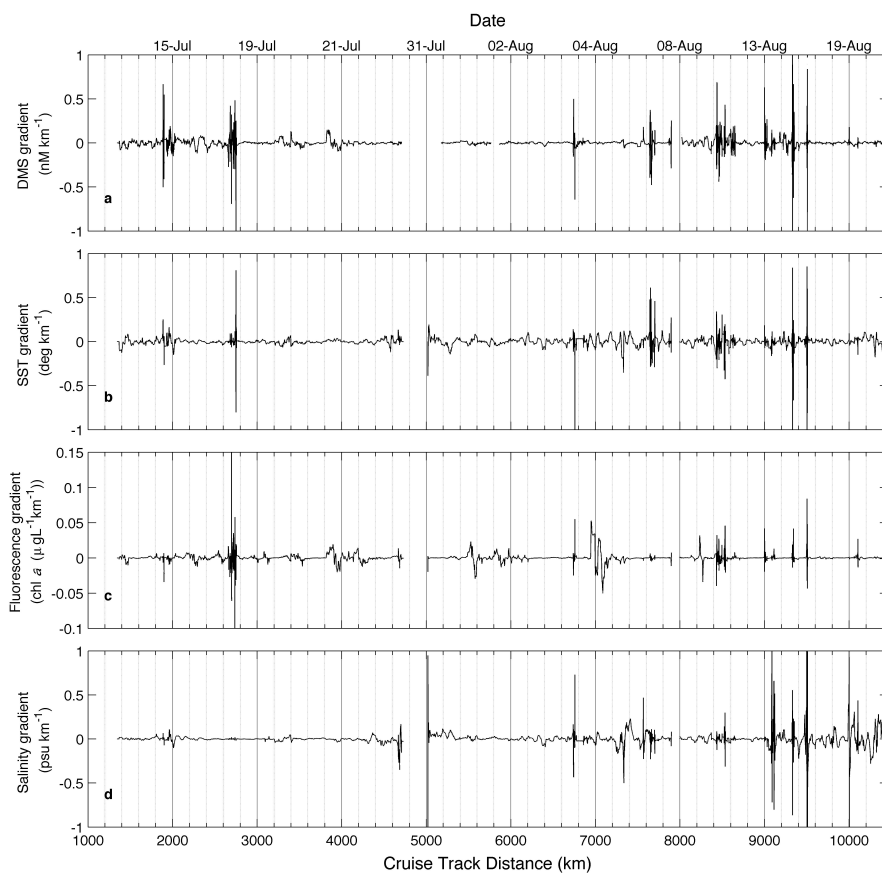
**Figure 4.** Spatial gradients in DMS and hydrographic variables.
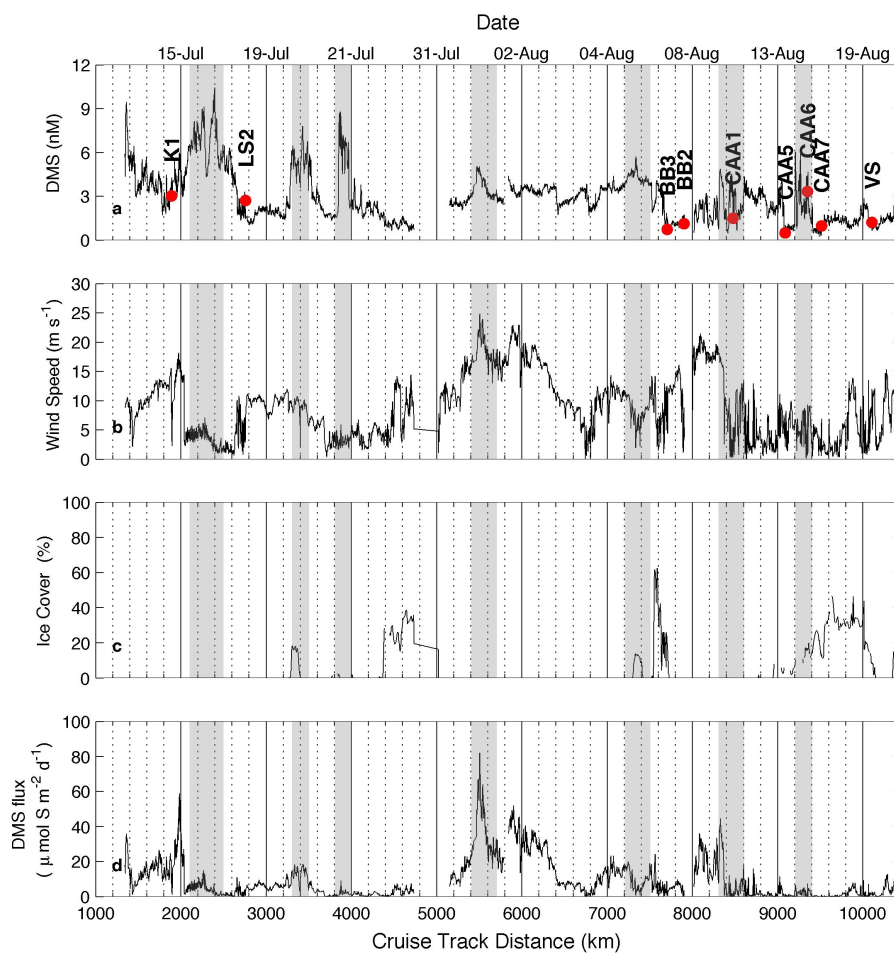
Figure 5. Distribution of DMS, wind speed, sea ice cover and sea-air DMS flux along the cruise track.
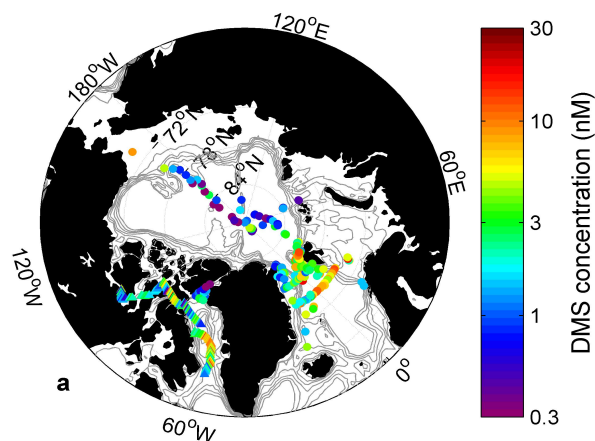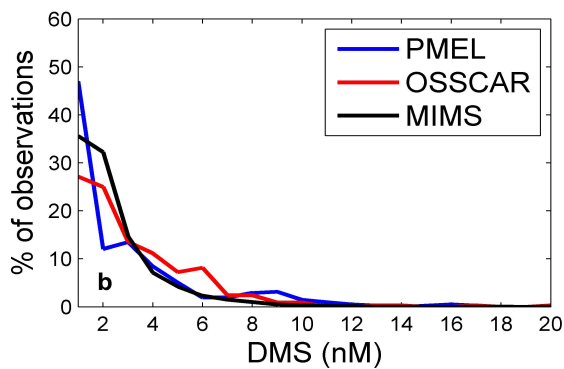
50

Figure 6. Comparison of OSSCAR- and MIMS-measured DMS from this study with existing data in the PMEL database

51